Tumor Biology and Immunology

Cancer Research

Perioperative, Spatiotemporally Coordinated Activation of T and NK Cells Prevents Recurrence of Pancreatic Cancer

Jennifer Brooks[1], Bettina Fleischmann-Mundt[1], Norman Woller[1], Julia Niemann[1], Silvia Ribback[2], Kristin Peters[2], Ihsan Ekin Demir[3], Nina Armbrecht[1], Guralp O. Ceyhan[3], Michael P. Manns[1], Thomas C. Wirth[1], Stefan Kubicka[1,4], Gunter Bernhardt[5], Mark J. Smyth[6], Diego F. Calvisi[2], Engin Gürlevik[1], and Florian Kühnel[1]

Abstract

Pancreatic ductal adenocarcinoma (PDAC) is a highly lethal and disseminating cancer resistant to therapy, including checkpoint immunotherapies, and early tumor resection and (neo)adjuvant chemotherapy fails to improve a poor prognosis. In a transgenic mouse model of resectable PDAC, we investigated the coordinated activation of T and natural killier (NK) cells in addition to gemcitabine chemotherapy to prevent tumor recurrence. Only neoadjuvant, but not adjuvant treatment with a PD-1 antagonist effectively supported chemotherapy and suppressed local tumor recurrence and improved survival involving both NK and T cells. Local T-cell activation was confirmed by increased tumor infiltration with $CD103^+CD8^+$ T cells and neoantigen-specific CD8 T lymphocytes against the marker neoepitope LAMA4-G1254V. To achieve effective prevention of distant metastases in a complementary approach, we blocked the NK-cell checkpoint CD96, an inhibitory NK-cell receptor that binds CD155, which was abundantly expressed in primary PDAC and metastases of human patients. In gemcitabine-treated mice, neoadjuvant PD-1 blockade followed by adjuvant inhibition of CD96 significantly prevented relapse of PDAC, allowing for long-term survival. In summary, our results show in an aggressively growing transgenic mouse model of PDAC that the coordinated activation of both innate and adaptive immunity can effectively reduce the risk of tumor recurrence after surgery, facilitating long-term remission of this lethal disease.

Significance: Coordinated neoadjuvant and adjuvant immunotherapies reduce the risk of disease relapse after resection of murine PDAC, suggesting this concept for future clinical trials. *Cancer Res; 78(2); 475–88. ©2017 AACR.*

Introduction

Pancreatic ductal adenocarcinoma (PDAC) is the fourth leading cause of cancer-related death and tumor resection is still the only potentially curative treatment (1). However, because PDAC patients are prone to develop systemic metastasis early in the course of the disease, the risk of tumor recurrence remains extraordinarily high with a 5-year survival rate of 10% after surgery alone and up to 25% with adjuvant chemotherapy, preferably gemcitabine (2). Initially introduced to reduce a large tumor burden to a resectable size, preoperative (neoadjuvant) treatments using chemotherapeutic agents or radiotherapy are now under investigation with the objective to interfere with the tumor vitality to minimize the risk of recurrence. A phase II study showed an improved 5-year survival rate to 36% when patients received gemcitabine and radiotherapy prior to pancreaticoduodenectomy (3). However, to achieve a sustained therapeutic benefit after tumor surgery for the vast majority of PDAC patients, further treatment options have to be considered to effectively prevent local tumor recurrence and outgrowth of distant metastases that are undetectable at the time of resection.

Cancer immunotherapies are a promising option to fight minimal residual and disseminated disease. Inhibition of T-cell checkpoints such as CTLA-4 or PD-1/PD-L1 has been shown to enable long-term responses in metastatic melanoma and renal cell cancer (4, 5), and their potential as (neo)adjuvant treatment is under investigation (6, 7). However, PDAC is much less responsive to single immunotherapies (8) most likely due to the uniquely immunosuppressive character of its tumor microenvironment. In general, the tumor microenvironment has been recognized to play an important role in cancer progression, therapy resistance, and in the control of tumor-directed cytotoxic lymphocyte responses thereby involving structural components and infiltrating immune cells of immunosuppressive character, including regulatory T cells, and several cell types of the myeloid lineage (9–12). In PDAC, it has been described that myeloid-derived suppressor cells are important for functional inactivation of T cells (13, 14). Macrophages and activated pancreatic stellate cells also contribute to exclusion of T cells from the tumor (15–17). A prominent characteristic of PDAC is the dense and hypovascular desmoplastic stroma that is responsible for therapy resistance and

[1]Department of Gastroenterology, Hepatology, and Endocrinology, Hannover Medical School, Hannover, Germany. [2]Institute of Pathology, University Medicine of Greifswald, Greifswald, Germany. [3]Department of Surgery, Klinikum Rechts der Isar, Technische Universität München, Munich, Germany. [4]Cancer Center Reutlingen, District Hospital, Reutlingen, Germany. [5]Institute of Immunology, Hannover Medical School, Hannover, Germany. [6]QIMR Berghofer Medical Research Institute, Herston, Australia.

Note: Supplementary data for this article are available at Cancer Research Online (http://cancerres.aacrjournals.org/).

Corresponding Author: Florian Kühnel, Hannover Medical School, Carl Neuberg Str. 1, 30625 Hannover, Germany. Phone: 49-511-532-3995; E-mail: kuehnel.florian@mh-hannover.de

doi: 10.1158/0008-5472.CAN-17-2415

is supposed to limit effective T cell access to tumor cells (18, 19). On the other hand, depletion of cancer-associated fibroblasts in experimental models of PDAC resulted in enhanced growth of undifferentiated tumors and reduced survival, suggesting that the stroma is also capable of constraining tumor expansion (20).

Nevertheless, the tumor epithelium itself remains an essential source for the release of tumor antigens and for cross-priming of tumor-directed T-cell responses as an important precondition for tumor response to checkpoint immunotherapies (21). After tumor resection, this important reservoir for induction of tumor-directed immune responses is no longer available. Consequently, perioperative therapies have to take into account the impact of primary tumor resection on the immune system for the design of clinical trials involving both neoadjuvant and adjuvant treatments. Whereas the presence of the tumor in the neoadjuvant phase could be exploited for innate immune activation and for priming effective adaptive responses, the adjuvant phase should primarily engage suitable means to combat minimal residual and disseminated disease.

In our study, we investigated the coordinated inhibition of (neo)adjuvant T-cell and natural killer (NK) cell immune checkpoints in the context of perioperative gemcitabine chemotherapy to prevent recurrence of PDAC. In a transgenic mouse model of locally induced, resectable PDAC, we found that neoadjuvant PD-1 blockade/gemcitabine suppressed local recurrence and improved survival in both NK cell and T-cell–dependent manner. However, neither neoadjuvant nor adjuvant PD-1 blockade was able to affect distant metastasis. To effectively address disseminated disease by a systemic NK cell activation, we additionally applied a CD96 blocking antibody following surgery. We found that neoadjuvant PD-1 blockade together with adjuvant CD96 inhibition was able to effectively prevent recurrence of PDAC after surgery, thus facilitating long-term survival. Our results demonstrate the therapeutic potential of coordinated immunotherapies in reducing the risk of tumor relapse and strongly encourage corresponding clinical studies.

Materials and Methods

Electroporation technique

Six- to 8-week-old p53fl/fl mice (Strain B6.129P2-Trp53^{tm1Brn}/J) were anesthetized with ketamine (100 mg/kg i.p.) and xylazine (10 mg/kg i.p.). Following laparotomy, the pancreatic tail was prepared for local plasmid injection. Plasmid DNA (50 μL of 0.5 μg/μL) was injected using a 27-gauge needle. The bleb was placed between the electrodes of a 5-mm diameter tweezers-type electrode. Four electric pulses for plasmid transfer were administered twice with 35-ms duration at 35 V and an interval of 500 ms using a CUY21SC Electroporator (NepaGene). The peritoneal cavity was washed three times with distilled water at 40°C and closed by suturing. Mice were kept under infrared light till awakening and then received metamizole (0.8 mg/mL) with the drinking water as postoperative analgesia.

Resection technique

Mice were anesthetized and laparotomized before the tumor-bearing pancreatic tail and spleen were prepared. Without touching the tumor, the blood vessel of the spleen was closed using a titanium ligating clip (Ethicon). After coagulation at 12 W with a 0.4-mm bipolar forceps (ERBE GmbH), the tissue was disconnected with a scissor. Then, the blood supply of the tumor-bearing pancreatic tail was also interrupted with a ligating clip. The adjacent tissue was coagulated at an adequate distance to tumor tissue and cut, thus facilitating surgical resection of tumor and spleen. The resection margin and remaining tissue were controlled to confirm complete tumor resection. The peritoneal cavity was washed three times with distilled water at 40°C and was closed by suturing. The mice were kept under infrared light until awakening. Mice received metamizole (0.8 mg/mL) with the drinking water as postoperative analgesia.

Plasmids

For sleeping beauty-mediated integration, the hyperactive transposase construct pPGK-SB13 was used (kindly provided by David A. Largaespada, University of Minnesota). As transposon plasmid for subsequent cloning procedures, we used the pT3/EF1α plasmid as backbone containing duplicated inverted repeats and an EF1α-promoter for transgene expression (Xin Chen, UCSF, Addgene plasmid 31789). For expression of Cre-recombinase, the plasmid pPGK-Cre-bpA was used (Klaus Rajewsky, MDC, Berlin, Addgene plasmid 11543). For delivery of transposons coding for KrasG12V, myrAkt2, and fLucL272A, respectively, we used the pT-KasG12V, pT-myrAkt2, and pT-EF1α-fLucL272A as described previously (16). For expression of the epitope tag of the neoantigen LAMA4-G1254V the LAMA4-G1254V encoding part L(MII) of the plasmid NL(MII)-NrasG12V described previously (22) was cloned into pT3/EF1α.

Treatment of mice

For neoadjuvant treatment, αPD-1 (150 μg/mouse diluted in physiological NaCl; clone RMP1-14, BioXcell) and gemcitabine (100 mg/kg bodyweight diluted in physiological NaCl) was administered intraperitoneally (i.p.) three times as indicated in the figures and figure legends. For adjuvant treatment, repeats of gemcitabine were administered weekly as indicated. αCD96 antibodies (clone 6A6 and clone 8B10 as previously described; ref. 23) were administered (i.p.) twice a week for six times in total using 250 μg/mouse/injection diluted in physiological NaCl. Mice in vehicle groups received isotonic NaCl solution (i.p.) as control.

For survival analysis, mice were sacrificed according to predefined termination criteria consistent with German regulations on animal welfare. At the time point of termination, metastasis and local recurrence were analyzed by macroscopic inspection and histologic examination of lung, liver, and pancreatic tissue.

Ethics approval for animal experiments

All *in vivo* experiments were conducted according to the German guidelines for animal care and use of laboratory animals (TierSchG). The experiments have been approved by the review boards of Hannover Medical School animal facility and by the responsible regional authorities (LAVES).

In vivo depletion of immune cells

During neoadjuvant treatment mice received additionally an anti-NK1.1 antibody (25 μg/mouse/injection for selective depletion of NK cells without depleting NKT cells; clone PK136, BioXCell) or an anti-CD8 antibody (75 μg/mouse, clone 53-6.72, BioXCell), or an anti-CD4 antibody (75 μg/mouse, clone GK1.5, BioXCell), or the corresponding isotype antibodies (clone MOPC-173, BioLegend). Depletion antibodies were administered three times (i.p.) simultaneously with neoadjuvant

treatment. For depletion of NK cells or CD8 T or CD4 T cells during adjuvant treatment, depletion antibodies, or isotype control antibodies were administered (i.p.) twice per week for six times in total. Following application of depletion antibodies, blood samples were drawn and efficacy of depletion was verified by FACS analysis.

Histologic analyses and immunohistochemistry

Tissue specimens were fixed with formalin and embedded in paraffin. For immunohistochemical analyses the following primary antibodies were used: anti–PD-L1 (ab131073, Abcam), anti-CK19 (14-9898-82, eBioscience), anti-E-Cadherin (ab76055, Abcam), and anti-CD155 (LS-B897-50, Biozol; HPA012568, Sigma). For diaminobenzidine (DAB) staining, sections were stained with the primary antibodies followed by corresponding biotin-coupled secondary antibodies (Invitrogen) and streptavidin–HRP (Invitrogen). Sections were then incubated with DAB (Zytomed) and nuclei were counterstained with hematoxylin. All immunohistochemical stainings were controlled with isotypes of the corresponding primary antibodies. For fluorescence analysis, secondary antibodies coupled to Alexa-Fluor488 (green) or Alexa-Fluor555 (red, Invitrogen) were used. Nuclei were counterstained with DAPI (Sigma).

Flow cytometry

Single-cell suspensions obtained from tumor tissue and spleen were analyzed after staining using a FACSCanto (BD Bioscience) instrument. For staining the following specifically conjugated antibodies were used: CD45.2-PerCP (clone: 104), CD11b-FITC (clone: M1/70), Gr1-PE (clone: RB6-8C5), CD8-APC; CD8-FITC (both clone:53-6.7), CD103-PE (clone: 2E7), CD4-FITC (clone: GK1.5), CD25-PE (clone: PC61.5) CD90.2-PerCP (clone: 30-H12), CD69-FITC (clone: H1.2F3), CD44-FITC (clone: IM7), CD11a-APC (clone: M17/4), Mult1-PE (clone: 5D10), Rae1y-PE (clone: CX1), and CD155-PE (clone: TX56). For intracellular staining of IFNy-APC (clone: XMG1.2), cells were treated with Brefeldin A (Biolegend) and then stimulated with peptide (irrelevant control (spectrin β), LAMA4(G1254V); ProImmune) and incubated overnight at 37°C and 5% CO_2. The next day, cells were stained with CD90.2-PerCP and CD8-FITC. After permeabilization with BD Cytofix/Cytoperm intracellular staining with an antibody for IFNγ-APC (clone: XMG1.2) was performed. All antibodies were obtained from Biolegend or eBioscience and datasets were analyzed using FlowJo software.

Luciferase activity assay from cell culture

Tumor cells were prepared from a primary tumor and stably transfected with pT3-EF1α-fLucL272A. Cells were then coincubated with different amounts of NK cells. NK cells were isolated with an NK cell Isolation Kit II (Miltenyi Biotec) according to the manufacturer's recommendations and NK cell purity was confirmed by FACS. The activity of luciferase was measured in supernatants and lysates after 4 hours of coincubation by luciferase-assay according to standard methods.

Human tissue specimens

A collection of formalin-fixed, paraffin-embedded PDAC and metastasis samples was used in the present study. Specimens were collected in the Institute of Pathology of the University of Greifswald with written informed consent from the patients. The studies were performed in accordance with the Helsinki Declaration and have been approved by the local ethics committee.

Statistical analysis

To determine statistical significance, log-rank (Mantel–Cox) test was used for survival curves. Fisher exact test (two-tailed) was used to compare the frequency of individuals with metastasis and disease recurrence. Student *t* test (unpaired, two-tailed) was used for comparison of two groups in all other experimental settings, values are given as mean ± SD. P values < 0.05 were considered statistically significant.

Results

Additional PD-1/PD-L1 inhibition of gemcitabine treatment after surgical removal of PDAC does not improve survival or burden of metastasis

To study the effect of immunotherapies on recurrence of PDAC after surgical tumor removal, we used a recently introduced transgenic mouse model of resectable PDAC (24). In p53fl/fl mice, a local, intrapancreatic injection and electroporation of oncogenic transposons coding for KrasG12V, myristoylated Akt2 (myrAkt2), and plasmids for sleeping beauty transposase and Cre recombinase lead to development of a locally restricted PDAC accessible for surgical resection (Fig. 1A). Twenty-two days after electroporation, tumors were resected and adjuvant treatments were initiated according to the treatment scheme shown in Fig. 1B. Adjuvant gemcitabine therapy preferably reduces local disease recurrence rather than affecting distant metastasis in human patients (2, 24). To achieve a more balanced suppression of local and distant metastasis to effectively prevent recurrence after tumor resection, we applied a systemic T-cell activation by adjuvant inhibition of the PD-1/PD-L1 axis. After adjuvant administration of gemcitabine (G) and a PD-1 blocking antibody, survival and metastasis patterns were investigated. Whereas adjuvant gemcitabine treatment significantly improved survival (Fig. 1C), simultaneous inhibition of the PD-1/PD-L1 checkpoint did not yield any additional therapeutic benefit. A remarkable reduction of local recurrence was observable after adjuvant gemcitabine whereas distant metastasis was not affected (Fig. 1D). In line with the survival results, the individual evaluation of metastasis patterns revealed that additional adjuvant treatment with αPD-1 did not affect the proportions of local recurrence and distant metastasis compared with adjuvant gemcitabine alone. These observations suggest that systemic T-cell stimulation following surgical removal of PDAC by inhibiting the PD-1/PD-L1 checkpoint is ineffective in treating disseminated disease in this model.

Neoadjuvant administration of αPD-1/gemcitabine improves tumor infiltration of tissue-resident $CD8^+CD103^+$ T cells and minimizes local tumor recurrence

Preoperative, neoadjuvant administration of chemotherapeutic agents with immunomodulatory activities may be capable of reactivating dormant tumor-directed immune responses and may help to restrain tumor dissemination and recurrence after tumor surgery. We investigated whether pre-activation of the T cell compartment prior to tumor removal could be an effective way to address distant metastases and recurrence. To test neoadjuvant treatments, we used αPD-1 or gemcitabine alone or the combination of both (αPD-1/G) and started drug administration 20 days after tumor induction according to the treatment scheme shown in Fig. 2A. At day 8 after start of therapy, the tumor was

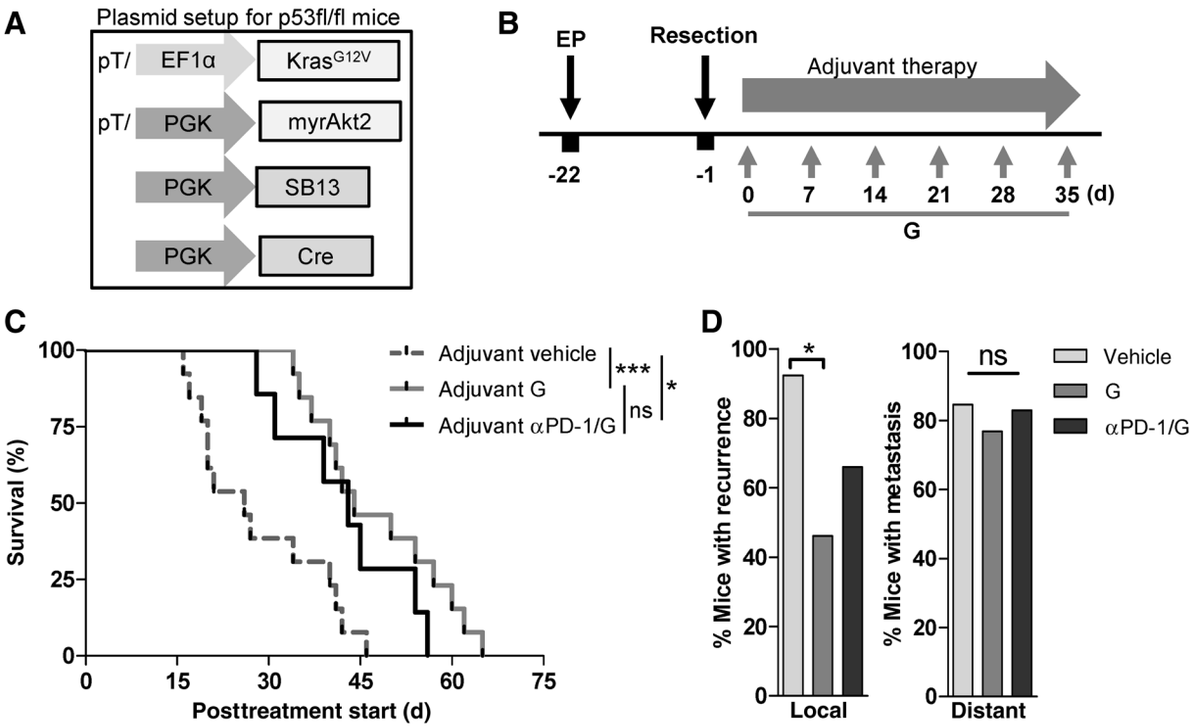

Figure 1.

Adjuvant treatment with αPD-1 and gemcitabine does not improve survival compared with adjuvant gemcitabine treatment alone. **A,** A local, resectable PDAC was established in mice using the electroporation technique. The applied plasmids for local injection and electroporation of the pancreatic tail are shown. Transposon-based plasmids for expression of KrasG12V and myristoylated Akt2 (myrAkt2), and plasmids for expression of sleeping beauty transposase SB13, and Cre recombinase were used in p53fl/fl mice, resulting in local tumor growth by p53 deletion and overexpression of oncogenic Kras and constitutive Akt2 activation. **B,** Twenty-two days after electroporation (EP), the tumor was surgically removed and mice received adjuvant treatments with αPD-1 and gemcitabine. The day after resection, treatment with gemcitabine (G), αPD-1/G, or vehicle was initiated. The schematic time line of applied adjuvant treatments is shown. Treatments were administered once a week for six times in total. Survival was monitored and metastasis was examined according to Material and Methods. Kaplan–Meier survival analysis comparing adjuvant treatment groups with mice that received vehicle ($n = 13$; ms, 26 d), G ($n = 13$; ms, 44 d), and αPD-1/G ($n = 7$; ms, 43 d) is shown in **C**. *, $P = 0.0251$; ***, $P = 0.0005$, log-rank (Mantel–Cox) test. The number of mice with local or distant disease recurrence was analyzed as shown in **D**. Detected local recurrence was 92.3% for vehicle, 46.2% for G, and 66.0% for the αPD-1/G group (*, $P = 0.0302$, Fisher exact test). Mice with metastasis in lung, liver, and peritoneum were summed up as a percentage of mice with distant metastasis: vehicle (84.6%), G (76.9%), αPD-1/G (83.0%).

resected and all mice further received adjuvant gemcitabine therapy. The survival analysis showed that the neoadjuvant administration of αPD-1 and gemcitabine resulted in significantly improved survival compared with single neoadjuvant therapies (Fig. 2B). Interestingly, neoadjuvant αPD-1/G led to a greatly reduced number of mice with local recurrent tumors, whereas αPD-1 or gemcitabine alone were less effective (Fig. 2C). A reduction of distant metastasis was not achieved by the neoadjuvant combination of treatments, suggesting that prolonged survival after neoadjuvant αPD-1/G is solely due to an improved local immune activation. Therefore, we analyzed tumor-infiltrating lymphocytes (TIL) focusing on CD8 T cells. We found that the total CD8 T-cell population in the tumor tissue was unaffected by different treatments (Supplementary Fig. S1). Further characterization of the intratumor CD8 T-cell population for several activation markers showed that neoadjuvant treatments neither affected the expression of CD69 and CD44, which are upregulated on activated T cells, nor expression of CD11a, a marker that is upregulated by CD8 T cells upon antigen experience (Supplementary Fig. S2). Recently, CD8 T cells expressing the surface marker CD103 have been described as tissue-resident and antigen-experienced tumor-specific CD8 TILs associated with a favorable prognosis in human patients (25, 26). Accordingly, we observed that particularly neoadjuvant αPD-1 treatment promoted tumor infiltration by $CD8^+CD103^+$ T cells (Fig. 2D). This effect was further enhanced after combination of αPD-1 and gemcitabine. Because CD103 interaction with E-Cadherin is an important requirement for cytotoxic functions of T-lymphocytes (27), we analyzed the expression of E-cadherin in murine samples of PDAC (Supplementary Fig. S3). Whereas the desmoplastic stroma did not show E-cadherin expression, the tumor epithelium was high in E-cadherin, indicating that tumors in this model are susceptible for cytotoxicity mediated by tumor-resident $CD8^+CD103^+$ T cells. Because we found that neoadjuvant application of αPD-1 alone is able to promote tumor infiltration with $CD8^+CD103^+$ T cells without a visible impact on survival, we looked for further immunomodulatory factors that determine T-cell activity in these tumors. It has been described that gemcitabine is able to promote T-cell–mediated antitumor activity by reducing numbers of myeloid-derived suppressor cells (MDSC) in the tumor microenvironment (28). Consistently, analysis of intratumor $Gr1^+CD11b^+$ cell population shows that gemcitabine alone or the combination

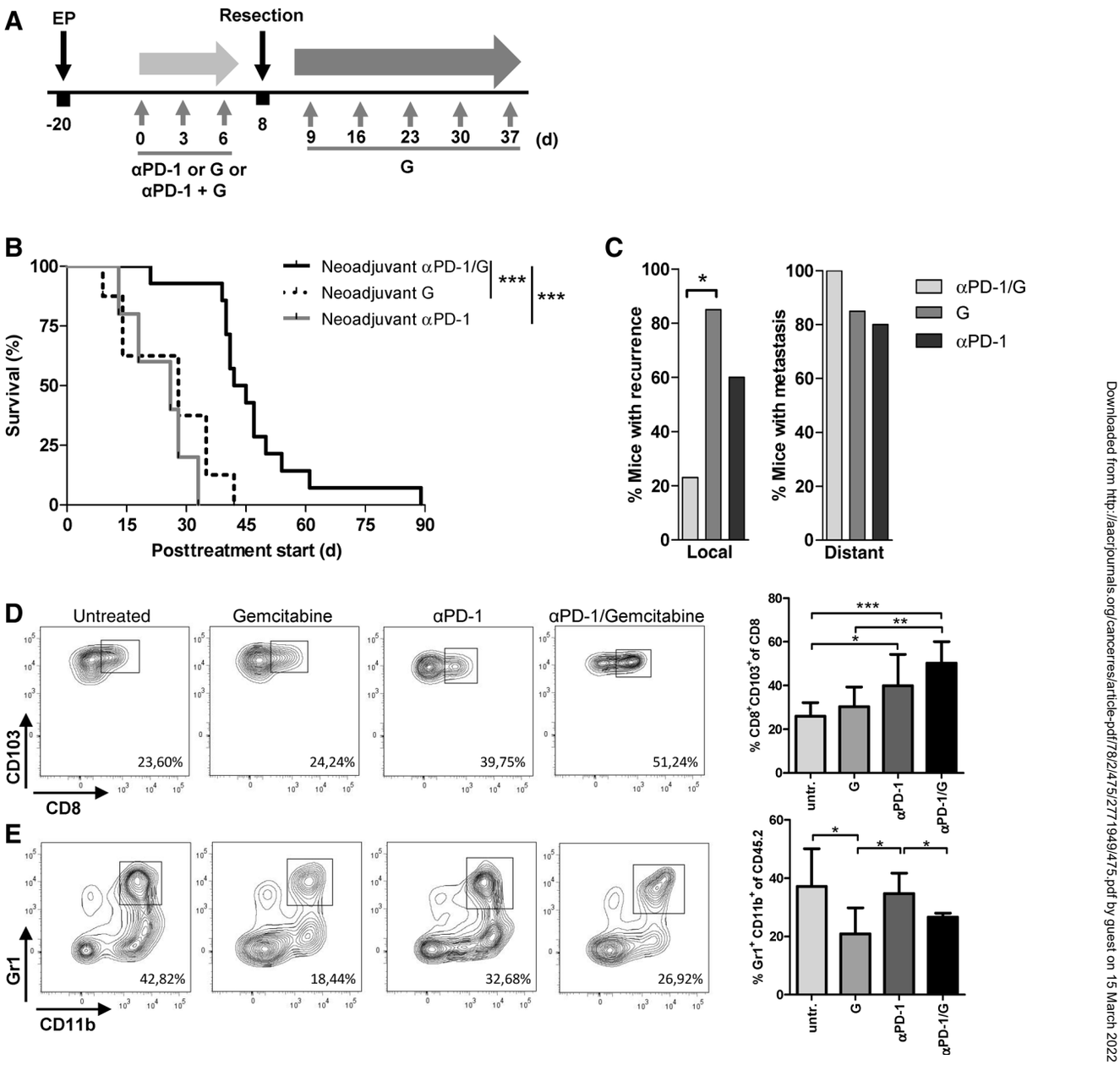

Figure 2.

Combined neoadjuvant treatment with αPD-1/G leads to elevated numbers of tumor-resident, $CD103^+CD8^+$ T cells and significantly improves local disease recurrence and survival. **A,** Tumor-bearing mice received neoadjuvant αPD-1 and/or gemcitabine. The figure shows the schematic timeline of neoadjuvant treatments. Twenty days following electroporation, a combination of αPD-1 and gemcitabine (PD-1/G) or the monotherapies were administered three times with an interval of three days. At day 8 of therapy, the tumor was surgically removed. After resection, adjuvant gemcitabine was given as standard therapy once a week for five times in total. **B** and **C** show survival and metastatic burden. **B,** Kaplan–Meier survival analysis of neoadjuvant-treated groups: αPD-1 ($n = 5$; ms, 26 d), G ($n = 8$; ms, 28 d), or αPD-1/G ($n = 13$; ms, 43.5 d). αPD-1 vs. αPD-1/G (***, $P < 0.0001$), G vs. αPD-1/G (***, $P = 0.0003$), log-rank (Mantel–Cox) test. **C,** Percentage of mice with local recurrence and distant metastases after combined neoadjuvant and adjuvant treatment. Local: αPD-1 (60%), G (85%), αPD-1/G (23%); *, $P = 0.0166$, Fisher exact test. Distant: αPD-1 (80%), G (85%), αPD-1/G (100%). At day 8 after therapy start, immune cells from primary tumors after treatment with αPD-1, G, αPD-1/G, or without treatment were isolated and analyzed with flow cytometry as shown in **D** and **E**. **D,** Cells were pregated for CD90.2. Contour plots of the $CD8^+CD103^+$ population (left) and quantification (right) are shown. G vs. αPD-1/G (**, $P = 0.0066$), untreated vs. αPD-1/G (***, $P < 0.0001$), untreated vs. αPD-1 (*, $P = 0.0237$); $n = 6$ per group, Student t test. **E,** Cells were pregated for CD45.2. Contour plots of $Gr1^+CD11b^+$ population (left) and quantification (right) are shown. Untreated ($n = 6$) vs. G ($n = 8$; *, $P = 0.0119$), G vs. αPD-1 ($n = 4$; *, $P = 0.0192$), αPD-1 vs. αPD-1/G ($n = 5$; *, $P = 0.0374$), Student t test.

with αPD-1 led to a significant drop of MDSC numbers in tumor tissue, suggesting a reduced level of immunosuppression in these groups (Fig. 2E). The analysis of $CD4^+CD25^+$ regulatory T cells in the tumor tissue showed that these cells were not affected by the different neoadjuvant treatments (Supplementary Fig. S4). Together, our observation that the neoadjuvant administration of the αPD-1/gemcitabine combination strongly prolonged survival compared with single treatments suggests a synergy of increased frequency of intratumor T cells in consequence of PD-1 blockade and attenuated immunosuppression by gemcitabine.

Neoadjuvant αPD-1/gemcitabine therapy stimulates tumor-directed, neoantigen-specific CD8 T-cell responses and triggers upregulation of PD-L1 in tumor tissue

To directly confirm the stimulation of adaptive immune responses against tumor-specific antigens, we established tumors expressing the neoepitope LAMA4-G1254V, which has been described previously (29). The applied plasmid setup for tumor establishment is shown in Fig. 3A. Corresponding to our previous therapeutic experimental settings (shown in Fig. 2A), tumor-bearing mice were treated with combined αPD-1/G, or single agents at days 0, 3, and 6, or were left untreated. Eight days following treatment start, neoepitope-directed CD8 T-cell responses were analyzed in tumor tissue and spleen by intracellular IFNγ staining. As shown in Fig. 3B, we found in $CD90.2^+CD8^+$ lymphocytes isolated from tumors in the αPD-1/G–treated group a significantly increased population of cells responding to the LAMA4-G1254V peptide. In contrast, all other groups showed no increased IFNγ response to this neoepitope (Fig. 3B and C). Investigation of the systemic LAMA4-G1254V–specific CD8 T-cell response by intracellular IFNγ staining of splenocytes revealed comparably low level of T-cell responses against this neoepitope in all groups (Fig. 3C). These results clearly demonstrate that only the combined αPD-1/gemcitabine treatment was capable of triggering substantial tumor-specific CD8 T-cell responses. Consistent with the prolongation of survival shown in the previous experiments, these results also provide a reasonable mechanistic argument for the therapeutic use of combined αPD-1/gemcitabine as neoadjuvant treatment for resectable PDAC. To further corroborate effective tumor-specific T-cell stimulation after αPD-1/gemcitabine treatment, we performed immunohistologic analysis of PD-L1 expression following αPD-1/gemcitabine or gemcitabine treatment alone (Fig. 3D). Local release of interferons as indicator of T-cell–mediated cytotoxicity upregulates PD-L1 on tumor cells. Samples of untreated human or mouse PDAC showed low expression of PD-L1 on the ductal tumor cells whereas stromal cells stained positive for PD-L1. In gemcitabine-treated mice PD-L1 expression on the tumor epithelium was also not elevated. In contrast, the αPD-1/G–treated tumor samples showed an intensive PD-L1 expression on the ductal tumor epithelium. To further characterize PD-L1 expressing cells, we additionally stained for CK19, a specific marker on hepatobiliary adenocarcinoma cells (Fig. 3E). The immunofluorescence images show a shift of PD-L1 expression from CK19-negative cells in tumors after treatment with gemcitabine alone (top) to PD-L1 expression on CK19-positive cells in the αPD-1/G–treated sample (bottom). Together, these findings demonstrate that combined αPD-1/gemcitabine treatment strongly promotes the generation of antitumoral CD8 T-cell responses.

Therapeutic benefit of neoadjuvant αPD-1/gemcitabine involves both CD8 and NK cells whereas only NK cells play a role in postoperative tumor control

The described experiments indicate a functional role of T lymphocytes in mediating the therapeutic benefit of neoadjuvant αPD-1/gemcitabine. To investigate the role of different immune cells during neoadjuvant and adjuvant treatment more in detail, we depleted CD8 T, CD4 T, or NK cells either preoperatively during neoadjuvant treatment with αPD-1/G or postoperatively during adjuvant treatment with gemcitabine (Fig. 4A). The results demonstrate that depletion of CD8 T cells or NK cells during neoadjuvant αPD-1/G treatment led in both cases to significantly reduced survival compared with the isotype control group (Fig. 4B). Furthermore, both depletions restored a high frequency of local disease recurrence (Fig. 4C) comparable with those seen in previous experiments (Fig. 1). Depletion of CD4 T cells did not affect the therapeutic effect on survival and local tumor recurrence. Distant metastasis was found in almost all individuals with no apparent differences between the groups. After neoadjuvant αPD-1/G treatment, depletion of CD8 T cells during continued adjuvant gemcitabine treatment did not affect survival or metastatic spread (Fig. 4D and E), suggesting that antitumor CD8 T cells play no role in control of the disease at this stage. Again, CD4 depletion had no effect compared with the isotype control group. Interestingly, depletion of NK cells during adjuvant treatment phase was able to impair survival and led to a significant increase in local tumor recurrence. To confirm a direct cytotoxic effect of NK cells, we established tumor cell lines from murine PDACs and generated luciferase-expressing derivatives. In an *in vitro* cell killing assay, luciferase-expressing tumor cells were incubated with isolated NK cells and luciferase activity released from killed cells was measured in the supernatant (Supplementary Fig. S5). We could show a target/effector ratio-dependent increase of luciferase activity confirming that the induced tumors are sensitive to direct NK cell–mediated cytotoxicity consistent with the survival results obtained in the depletion studies.

CD155 is highly expressed on tumor cells, representing a promising target for NK cell–based immunotherapeutic approaches

Next, we analyzed NK cell ligands on tumor cells derived from the used model. The results show that well-known NK cell ligands such as Rae1γ and Mult1 were not expressed (Fig. 5A). Then, we investigated expression of CD155, an NK cell ligand that is also referred to as poliovirus receptor protein. CD155 is an immunoglobulin-like cell adhesion factor involved in transendothelial cell migration of leukocytes and contributes to the regulation of NK cell activity by its ability to bind to CD226, TIGIT, and CD96 on the surface of NK cells (30, 31). It has been shown that CD155 is highly expressed on tumor cells including human pancreatic cancer (31, 32). In our model, the results revealed a high expression of CD155 on tumor cells derived from primary tumor material as well as of recurrent tumors and liver metastasis (Fig. 5A). Analysis of specimens from disseminated human PDAC confirmed that CD155 is indeed expressed in the primary tumor and PanIN lesions as well as in liver- and lymph node metastasis (Fig. 5B). An expression in the primary tumor was found in 56% of the examined samples, PanINs only showed a positive staining in 4 out of 11 samples. The examination of metastasis revealed a positive CD155 staining in 54.5% of liver and in 70% of lymph node metastasis (Fig. 5C). Because binding of CD155 to CD96 on

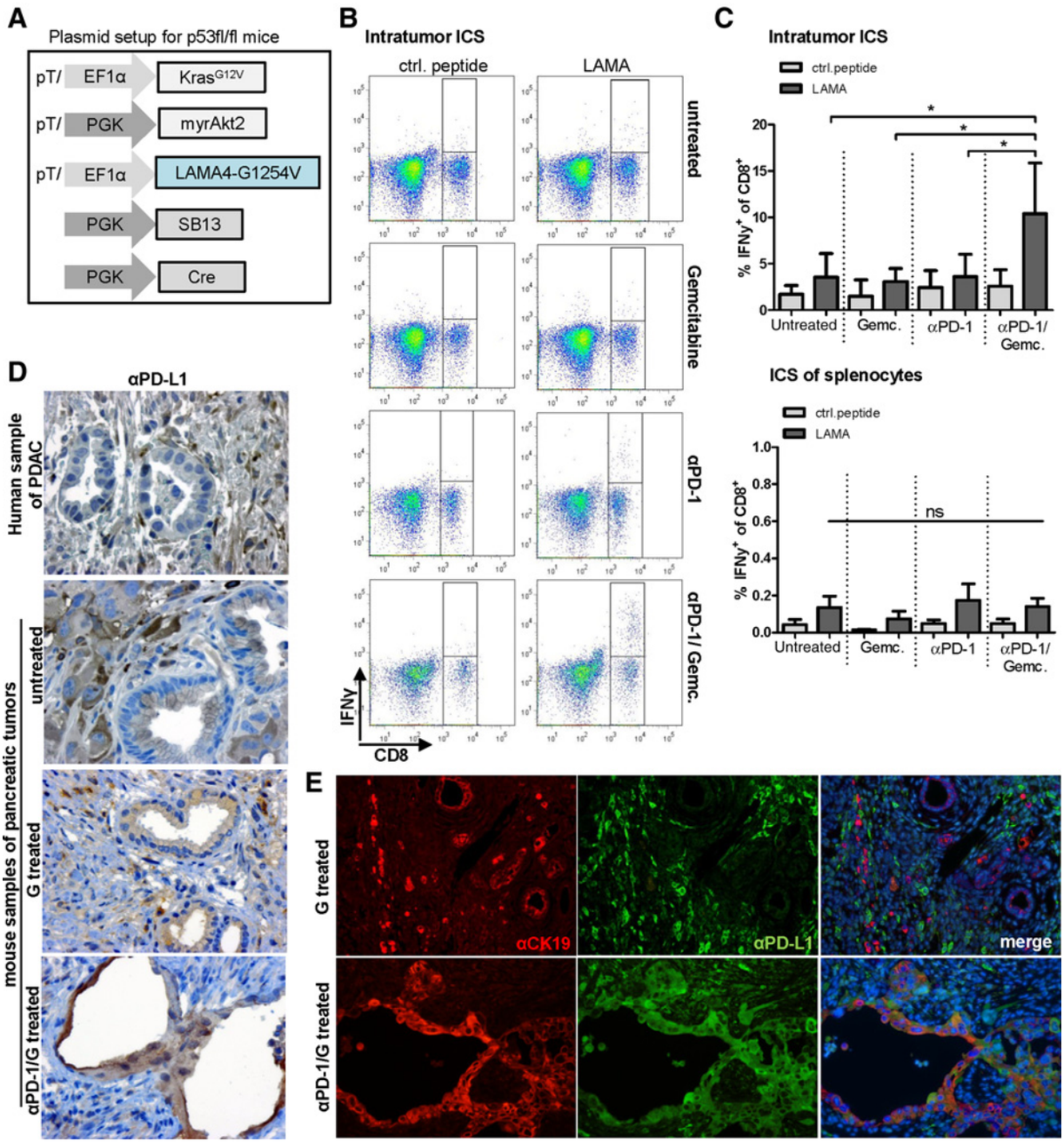

Figure 3.

Neoadjuvant treatment using combined αPD-1 and gemcitabine elicits local tumor-specific CD8 T-cell responses and triggers expression of PD-L1 on tumor cells. **A,** Plasmid setup for induction of PDAC expressing a tumor-associated neoantigen. Plasmids containing KrasG12V, myrAkt2, and LAMA4-G1254V epitope transposons, and plasmids for expression of SB13 transposase and Cre recombinase were used for electroporation in p53fl/fl mice. This genetic setup reflects a p53-deleted PDAC overexpressing oncogenic Kras and myrAkt2 that additionally express the neoantigenic epitope LAMA4(G1254V). **B,** After neoadjuvant treatment with combined αPD-1/G or αPD-1 and G alone, immune cells from tumor tissue and spleen were isolated at day 8 after treatment start. Tumor-bearing, but untreated, mice served as control. After stimulation with irrelevant peptide (ctrl.) or LAMA4(G1254V) peptide, cells were stained for CD90.2, CD8, and subjected to intracellular IFNγ staining. Representative dot plots of intratumor IFNγ$^+$ CD8 T cells after pregating for CD90.2 are shown for all groups. **C,** Quantitative analyses of IFNγ$^+$ CD8 T cells after stimulation. Analyses of intracellular IFNγ staining of the immune cells isolated from tumor tissue (top) or from spleen (bottom) are shown. Untreated vs. αPD-1/G (*, $P = 0.0179$), G vs. αPD-1/G (*, $P = 0.0286$), αPD-1 vs. αPD-1/G (*, $P = 0.0169$); Student t test (untreated, $n = 6$; G, $n = 5$; αPD-1, $n = 5$; αPD-1/G, $n = 7$). **D,** Immunohistochemical staining of PD-L1 in a tumor specimen derived from a human PDAC patient (top) and in mouse samples of pancreatic tumors treated with gemcitabine, αPD-1/G, or untreated. Magnification, ×100. **E,** Immunohistochemical analysis of CK19 and PD-L1 coexpression in gemcitabine or αPD-1/G–treated murine pancreatic tumors. Magnification, ×100.

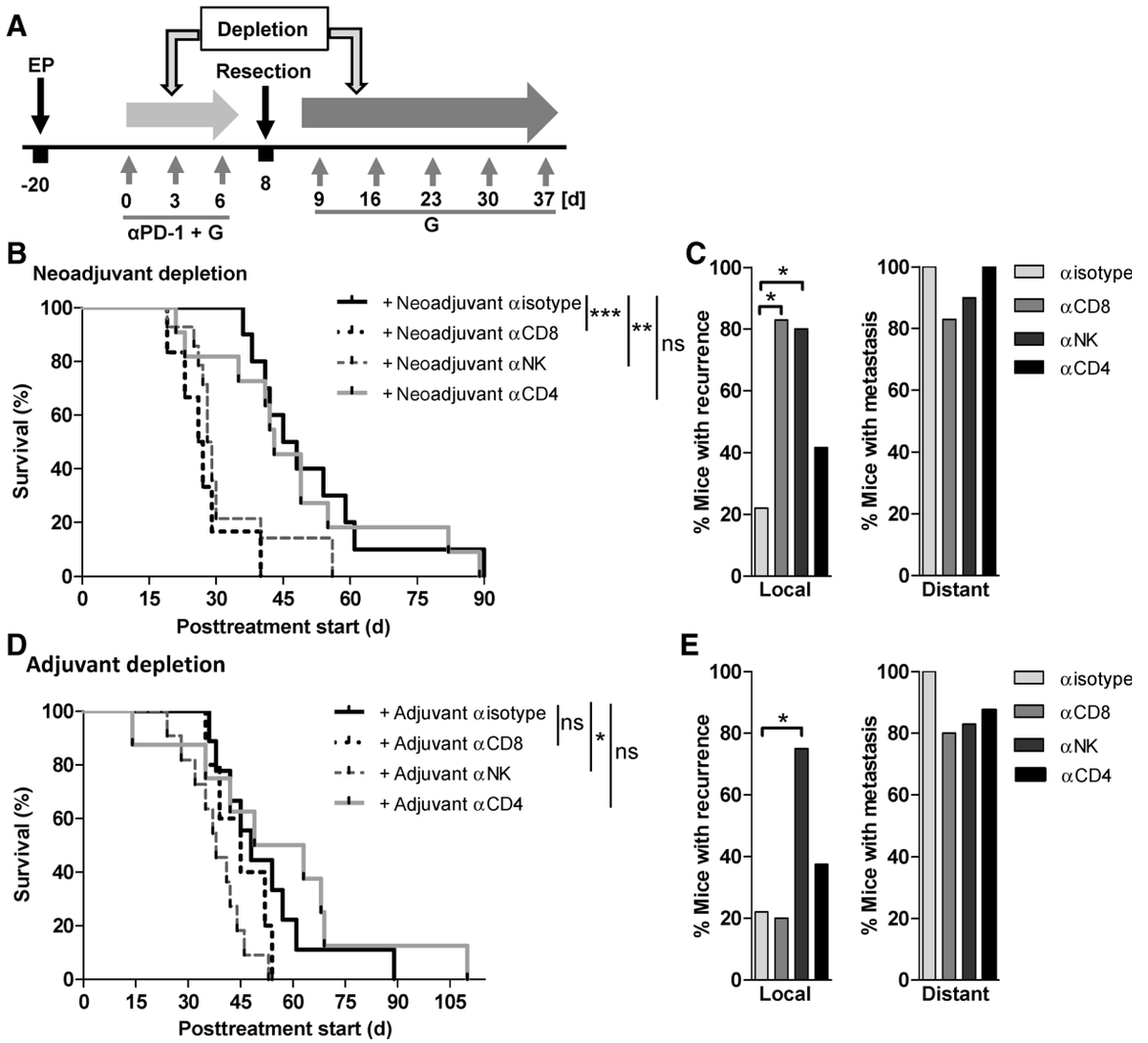

Figure 4.

During neoadjuvant treatments with αPD-1 and gemcitabine, both CD8 T and NK cells play an important role in effective elimination of local recurrence. **A,** The role of specific immune cell population in neoadjuvant treatments with αPD-1 and gemcitabine (G) was investigated by antibody depletion studies. The figure describes a schematic overview of applied antibody-mediated immune cell depletion during neoadjuvant or adjuvant treatment phases with neoadjuvant αPD-1/G and adjuvant gemcitabine treatment. **B** and **C,** At the same time of neoadjuvant treatment with αPD-1/G depletion, antibodies for CD4 T, CD8 T, or NK cells were administered. All mice received adjuvant G. Survival was monitored and investigated by Kaplan–Meier analysis as shown in **C**. Isotype ($n = 10$; ms, 46.5 d), αCD8 ($n = 6$; ms, 26.5 d), αNK1.1 ($n = 10$; ms, 28 d), αCD4 ($n = 12$; ms, 43 d). **, $P = 0.0046$; ***, $P = 0.0001$; log-rank (Mantel–Cox) test. The impact of CD4 T-cell, CD8 T-cell, and NK-cell depletion on incidence of local recurrence and metastatic dissemination was analyzed as shown in **C**. Local: Isotype (22%) vs. αCD8 (83%); *, $P = 0.04$; isotype vs. αNK1.1 (80%); *, $P = 0.023$; αCD4 (41%). Distant: Isotype (100%), αCD8 (83%), αNK1.1 (90%), αCD4 (100%). Fisher exact test. **D** and **E,** Mice received neoadjuvant αPD-1/G and adjuvant gemcitabine treatment. Simultaneously, adjuvant G CD4 T, CD8 T, or NK cells were depleted and the impact on survival and metastatic dissemination was monitored. **D**, Kaplan–Meier survival analysis. Isotype ($n = 9$; ms, 48 d), αCD8 ($n = 5$; ms, 45 d), αNK1.1 ($n = 12$; ms, 38 d), αCD4 ($n = 8$; ms, 56 d). *, $P = 0.0103$, log-rank (Mantel–Cox) test. **E**, The proportion of local recurrence and metastases in mice after depletion during adjuvant treatment phase. Local: Isotype (22%) vs. αCD8 (20%) ns, nonsignificant; isotype vs. αNK1.1 (75%); *, $P = 0.03$; αCD4(37%). Distant: Isotype (100%), αCD8 (80%), αNK1.1 (83%), αCD4 (87%). Fisher exact test.

NK cells inhibits their activation, targeting the CD96/CD155 axis with inhibitory antibodies has already shown antitumor effects in mouse syngeneic models of melanoma, prostate, and breast cancer (33). Therefore, interfering with the CD96/CD155 NK cell checkpoint represents a promising target for adjuvant NK cell activation in PDAC. To investigate the interference with the CD96/CD155 interaction and to stimulate the NK cell activity, we used two different αCD96 antibodies, clones 6A6 and 8B10, differing in their capacity to block CD96 binding to CD155. Only clone 6A6 but not 8B10 is able to interfere completely with CD155 coupling (34). In a first trial, these antibodies were used as a postoperative additional treatment to supplement the

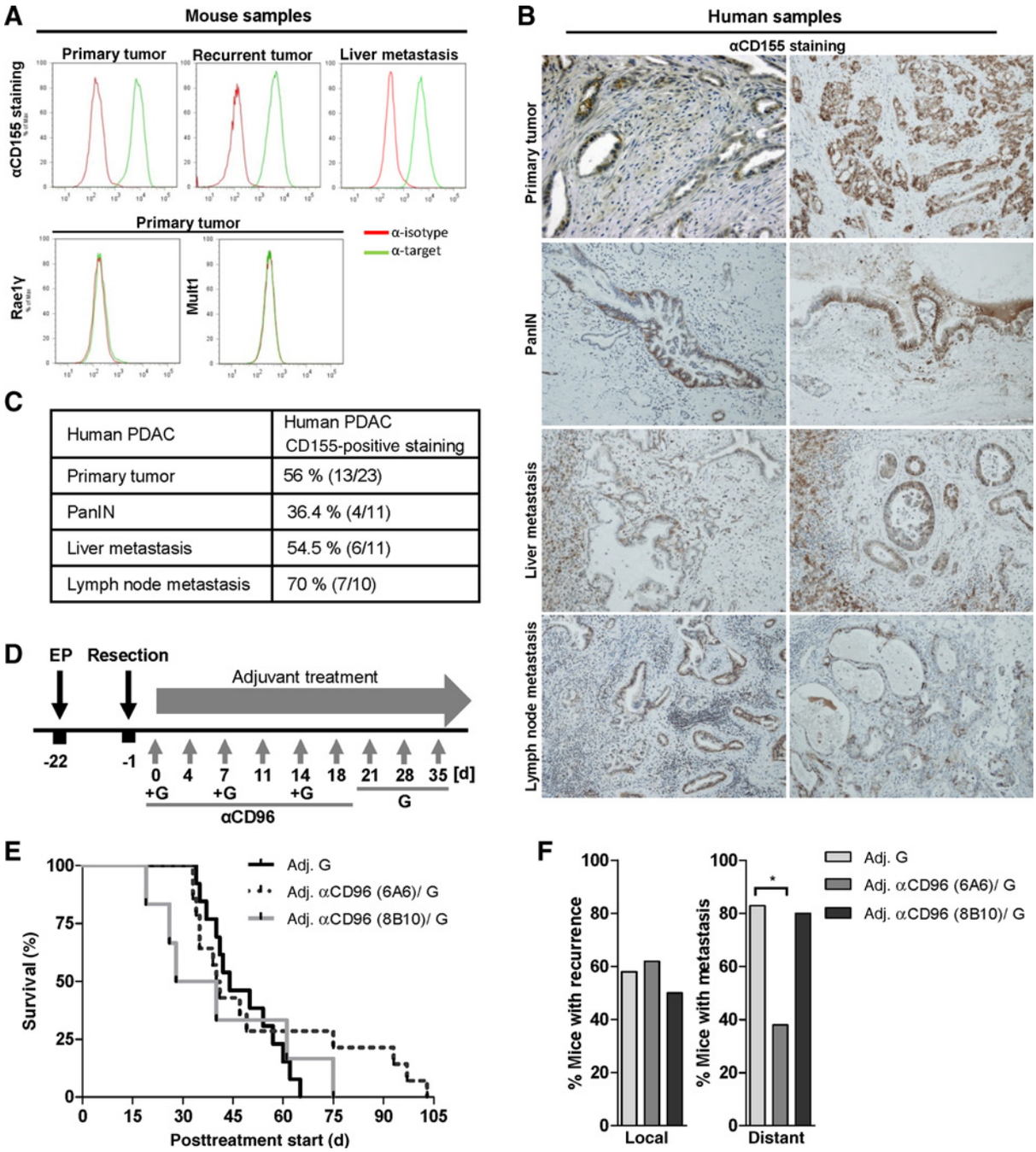

Figure 5.

Adjuvant αCD96 significantly reduces metastatic dissemination and results in survival benefit. **A,** Tumor cells were harvested and cultured after isolation from electroporation-induced primary PDAC and expression of NK-cell ligands CD155, Mult1, and Rae1γ was investigated by flow cytometry. Flow cytometric staining of CD155 of cultured tumor cells derived from primary tumor was compared with cultured cell isolates derived from recurring tumor or liver metastases (top row). Expression of Mult1 and Rae1γ is shown in the bottom row. **B,** Immunohistochemical analysis of CD155 expression on samples of primary tumor, PanIN, liver metastasis, and lymph node metastasis derived from human patients. Magnification, ×100. **C,** Table summarizing the results of immunohistochemical staining of CD155 in human PDAC specimens and metastasis. **D,** Schematic time line of αCD96 combination with gemcitabine in the adjuvant treatment approach. Twenty-one days after electroporation, the tumor was resected and 1 day later the treatment with αCD96 and gemcitabine started. αCD96 (6A6 or 8B10) was administered twice a week for six times in total, whereas gemcitabine was administered once a week for six times in total. The survival and metastatic disease was monitored as shown in **E** and **F**. **E,** Kaplan–Meier survival curve showing the effect of additional αCD96 to adjuvant gemcitabine. G ($n = 13$; ms, 44 d), αCD96(6A6)/G ($n = 14$; ms, 40.5 d), αCD96(8B10)/G ($n = 6$; ms, 34 d). **F,** Percentage of mice with local recurrence and distant metastases after adjuvant treatment. Local: G (58%), αCD96(6A6)/G (62%), αCD96(8B10)/G (50%). Distant: G (83%) vs. αCD96(6A6)/G (38%); *, $P = 0.041$; αCD96(8B10)/G (80%); Fisher exact test.

cytostatic activity of adjuvant gemcitabine according to the treatment scheme shown in Fig. 5D. In the majority of individuals, additional NK cell stimulation did not yield any life prolongation (Fig. 5E). The clone 8B10 did not yield a significant therapeutic benefit consistent with unaffected patterns of metastasis (Fig. 5F). Nevertheless, the results demonstrated that the αCD96 (6A6) antibody led to prolonged survival in a number of mice. Although prolongation of survival was not significant, we found a significantly reduced frequency of mice with distant metastases confirming the systemic antimetastatic activity of this antibody in this PDAC model. Most importantly, these findings promised that αCD96-mediated suppression of distant metastases following tumor surgery could optimally supplement the observed local immune activation by neoadjuvant PD-1 inhibition to effectively prevent recurrence of PDAC.

Neoadjuvant αPD-1/gemcitabine, followed by adjuvant NK cell–directed immunotherapy, facilitates cure after resection of PDAC

To realize a coordinated immunotherapy during tumor resection, we started treatment of tumor-bearing mice with neoadjuvant αPD-1/G 20 days after tumor induction before the tumor was removed at day 8 of therapy. After surgical tumor removal, mice received an adjuvant treatment of six subsequent applications with αCD96 and additional cytostatic gemcitabine treatment once weekly according to the treatment scheme in Fig. 6A. To confirm the contribution of NK cell activation, a further treatment group received an NK cell–depleting antibody. Survival monitoring demonstrated that the adjuvant treatment with αCD96 (6A6) after neoadjuvant αPD-1/G (and continued gemcitabine) resulted in a significantly improved survival compared with the same treatments without αCD96 (Fig. 6B). Even in this challenging and extremely aggressive tumor model, a relevant proportion of long-term survivors was observed confirming that coordinated immunotherapy with neoadjuvant αPD-1 blockade and adjuvant NK cell stimulation in addition to conventional gemcitabine treatment can cure resectable PDAC. Treatment success was completely abrogated when NK cells were depleted during the postoperative treatment phase, confirming the important role of these cells in disease control in general and, particularly, in controlling distant metastasis. The crucial relevance of fighting distant metastasis in achieving long-term survival was further confirmed by the observation that addition of the alternative antibody αCD96 (8B10) had actually a positive effect on survival but was unable to achieve any long-term survival. The analysis of metastasis patterns at the time of sacrifice showed that the antitumor activity of the treatment without αCD96 (6A6) was preferably effective against local recurrence, suggesting that distant metastasis was the most probable life-limiting factor (Fig. 6C, left). In contrast, adding αCD96 (6A6) significantly prevented distant recurrence (Fig. 6C, right), which in turn resulted in a more balanced antitumor effect on both local and distant tumors and a substantial survival benefit. Effective suppression of distant metastasis was dependent on αCD96 (6A6)-dependent NK cell activation as shown by specific depletion of NK cells.

In summary, our results show that neoadjuvant αPD-1/gemcitabine treatment for suppression of local disease recurrence can be ideally combined with NK cell activation to reduce distant metastasis. This spatiotemporally coordinated immunotherapeutic approach to support conventional gemcitabine treatments is a promising strategy to significantly improve long-term survival after resection of PDAC in humans.

Discussion

Adjuvant systemic chemotherapy is recommended to reduce the risk of recurrence of PDAC, but clinical benefit is limited. Before and after resection of a primary tumor, systemic treatments accompanying tumor surgery are facing different challenges regarding tumor burden and microenvironment. Furthermore, surgical stress can transiently suppress antitumor T cells and NK cells, thus promoting dissemination and recurrence (35, 36). Future therapies should therefore complement the surgical removal of the bulk tumor mass in a coordinated manner to achieve optimal immunoactivation and to facilitate effective elimination of residual tumor cells at local and distant sites.

In our study, we addressed the specific demands before and after surgical tumor removal of PDAC by adapted immunotherapies to develop a treatment that optimally complements gemcitabine therapy. This was investigated in a murine model of PDAC with a resectable primary tumor and early metastasis, driven by oncogenic KrasG12V, activated Akt2, and dysfunctional p53. In this model, a spatiotemporally coordinated immunotherapy combined with gemcitabine yielded a substantial therapeutic benefit and significantly decreased the risk of tumor recurrence. The chosen immunotherapeutic strategy included T-cell activation by neoadjuvant inhibition of PD-1 prior to surgery followed by adjuvant NK cell activation by blocking CD96. The treatment facilitated long-term survival even in this aggressive model whereas no long-term survivor was observable in control groups receiving (neo)adjuvant monotherapies, or adjuvant combinations, respectively. Our observations clearly confirm the potential of such coordinated immunotherapies accompanying tumor resection.

Though palliative treatment of PDAC with checkpoint inhibitors is rather inefficient, several findings do not exclude immunoreactivity. Inflammation is involved in carcinogenesis of PDAC and has been recognized as therapeutic target (37–40). In patients, PDAC contains a repertoire of tumor-reactive T cells similar to more immunogenic tumors, such as melanoma (41). However, immune cell infiltrates in PDAC are effectively suppressed and immobilized by the desmoplastic stroma representing more than 80% of the total tumor mass. Consistently, it has been recently demonstrated that targeting the integrity of the desmoplastic stroma renders PDAC responsive to PD-1 antagonists (42). As an example of innate immunoreactivity of PDAC, we previously showed that adjuvant gemcitabine promoted local NK cell activity, thus lowering the risk of local tumor recurrence (24).

In this study, we surprisingly found that additional adjuvant application of a PD-1 blocking antibody neither affected recurrence patterns nor improved survival compared with gemcitabine monotherapy. A reason for this could be the presumably low neoantigenic load in our model, which is driven by strong oncogenes and develops within a short time. The neoantigenic load provides targets for tumor-directed CD8 T cells and is being regarded as a potential predictor of tumor response to checkpoint immunotherapies (43, 44). Our findings therefore do not argue against adjuvant PD-1 blockade. A further suitable explanation for the failure of adjuvant checkpoint inhibition in our experiments

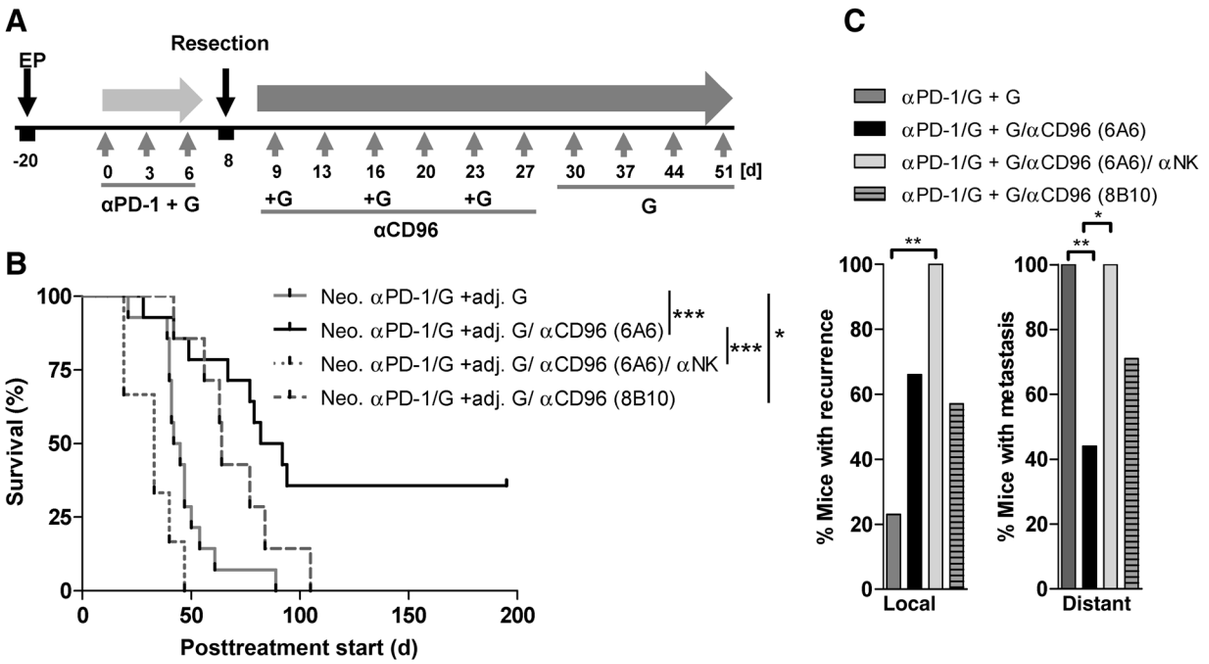

Figure 6.

Combination of adjuvant αCD96 with neoadjuvant αPD-1/G treatment reduces distant metastasis and results in long-term cure. **A,** Schematic overview of combination of neoadjuvant αPD-1/G and adjuvant αCD96/G treatment. Twenty days after electroporation, αPD-1/G was administered every 3 days for three times. After resection (8 days after treatment start), adjuvant αCD96 was given twice a week for six times in total. Additional gemcitabine was administered once weekly for 7 weeks. In one group, NK cells were depleted adjuvant simultaneously to αCD96/G treatment by administration of depletion antibodies two times per week for three weeks. Analysis of survival is shown in **B** and metastatic spread is shown in **C**. **B,** Kaplan–Meier survival curve showing the effect of additional αCD96 in the adjuvant treatment phase of neoadjuvant αPD-1/G and adjuvant G. αPD-1/G ($n = 14$; ms, 43.5 d) vs. αPD-1/αCD96(6A6)/G ($n = 14$; ms, 87 d); ***, $P = 0.0002$; αPD-1/G vs. αPD-1/αCD96(8B10)/G ($n = 7$; ms, 64 d); *, $P = 0.0287$; αCD96(6A6)/G vs. αPD-1/αCD96(6A6)/G/αNK1.1 ($n = 6$; ms, 33 d); ***, $P < 0.0001$. Log-rank (Mantel–Cox) test. **C,** Quantification of metastatic spread after combined neoadjuvant αPD-1/G and adjuvant αCD96/G treatment. Local recurrence: αPD-1/G (23%) vs. αPD-1/αCD96 (6A6)/G/αNK1.1 (100%); **, $P = 0.0031$; αPD-1/αCD96(6A6)/G (66%); αPD-1/αCD96(8B10)/G (57%). Distant: αPD-1/G (100%) vs. αPD-1/αCD96(6A6)/G (44%); **, $P = 0.0048$; αPD-1/αCD96(6A6)/G vs. αPD-1/αCD96(6A6)/G/αNK1.1 (100%); *, $P = 0.0440$; αPD-1/αCD96 (8B10)/G (71%). Fisher exact test.

could be the withdrawal of the tumor as source of tumor antigen. The importance of generating T-cell responses as a substrate for subsequent checkpoint blockade has been confirmed in murine models of PDAC and in patients who received a neoadjuvant vaccine application prior to surgery and checkpoint inhibition (45, 46).

Consistently, we demonstrated that only the neoadjuvant combination of gemcitabine and a PD-1 inhibitor improved survival. Interestingly, we observed that intratumor $CD103^+CD8^+$ T-cell frequencies increased after neoadjuvant αPD-1 monotherapy without a therapeutic benefit, suggesting that additional factors are involved. It has been shown that gemcitabine interferes with the immunosuppressive myeloid compartment in favor of effective immune cell priming for subsequent checkpoint inhibition (28). Consistently, we found in our model after neoadjuvant αPD-1/G treatment, a significant reduction of $CD11b^+Gr1^+$ myeloid-derived suppressor cells in parallel with a maximum of tumor-resident $CD103^+CD8^+$ T cells. These results were further confirmed because we only observed a strong intratumor infiltration of CD8 T cells against the neoepitope LAMA4-G1254V in mice receiving the neoadjuvant combination of gemcitabine and PD-1 inhibition. In this group, tumor-directed T-cell immunity was demonstrated by enhanced expression of PD-L1 on the tumor epithelium. PD-L1 is expressed by tumor cells in response to IFNγ released by activated T cells (47) and its expression has been suggested as a surrogate marker for tumor response to checkpoint inhibition (48, 49). Our observations are in line with recent findings in murine models of breast cancers describing that neoadjuvant application of checkpoint inhibitors was superior compared with adjuvant treatments (6). However, Liu and colleagues found that distant metastases were effectively eradicated by activated T cells, whereas we found only a locally restricted effect of T-cell activation by neoadjuvant gemcitabine/PD-1 blockade, suggesting significant differences in the tumor microenvironment and therapeutic demands in the tumor models under investigation.

PDAC metastasis is highly resistant to systemic chemotherapy attributable to stem cell–like features at early stages (50) and, with increasing size, to established resistance features of mature PDAC including desmoplastic stroma and hypovascularity (19, 51). Because activated T cells did not affect distant metastasis in our model, we considered alternative effector immune cells for this purpose such as NK cells. CD155 is abundantly expressed on epithelial cells including tumors, and it is known that the interaction of CD155 with the NK cell receptor CD96 inhibits NK cell function by negative regulation of the cytokine response, and it has been shown that $CD96^{-/-}$ mice are more resistant to carcinogenesis and experimental metastasis (30, 52). Accordingly,

therapeutic NK cell targeting using the CD96 antibody 6A6 effectively inhibits experimental metastasis in murine tumor models of melanoma, breast, and prostate cancer (33). It has been recently shown that CD155 is highly expressed in human pancreatic cancer and that CD155 expression is associated with poorer prognosis (31, 32). Consistent with these findings, we detected abundant CD155 expression in patient-derived samples. Moreover, strong CD155 was not only found on primary PDAC but also in PanINs, and metastases in liver and lymph nodes, confirming that targeting the CD96/CD155 axis for systemic NK cell stimulation is a promising strategy to address metastasis. Accordingly, we found CD155 expressed in primary tumors and metastases in our mouse model. Adjuvant application of the anti-CD96 antibody 6A6, which is capable of completely blocking CD96/CD155 interaction (34) reduced the metastatic burden significantly without yielding a survival benefit. However, we found that sequential immunotherapy with neoadjuvant PD-1 blockade followed by adjuvant CD96 inhibition resulted in a significant number of long-term surviving mice after tumor surgery and conventional gemcitabine treatment. Long-term survival was abrogated by NK cell depletion, confirming the essential role of systemic postoperative NK cell stimulation. CD96 binds to CD155 and nectin-1, and it is expressed by NK cells, T cells, and a subpopulation of B cells. In humans, but not in mice, CD96 is expressed in two splice variants that bind to CD155 (34). Variant V2 differs from variant V1 in the extracellular domain 2 and binds stronger to CD155 than V1. Furthermore, V2 is the most predominantly expressed variant in human leukocytes and corresponds to mouse CD96 (34). Nevertheless, it should be considered for translation in human patients to use antibodies that block the interaction of both splice variants with CD155 to achieve optimal efficacy. This could most likely be accomplished by an antibody that binds to extracellular domain 1 of CD96, which is the most relevant for CD155 binding and which is identical in both variants. It has been recently demonstrated that CD96 and CD226 expression on NK cells can be altered in patients with pancreatic cancer that is possibly related to increased NK-cell dysfunction (31). Whereas Peng and colleagues detected a decreased number of CD96-positive NK cells in pancreatic cancer patients, mean fluorescence intensity on these cells was equivalent to healthy controls. Nevertheless, it might be necessary to know whether patients with reduced CD96 may actually benefit from blocking the CD96/CD155 interaction.

In summary, our data demonstrate that optimal adaptation of immunotherapies to specific needs in the preoperative and postoperative situation effectively prevents tumor recurrence and enables complete cure after surgical removal even in case of extremely lethal tumors such as PDAC. These promising findings generally encourage the clinical exploration of spatiotemporally coordinated combinations of T cell– and NK cell–directed immunotherapies for the treatment of patients undergoing tumor surgery.

Disclosure of Potential Conflicts of Interest

S. Kubicka has received honoraria from speakers bureau of Amgen, Roche, Sanofi, Bayer, and Merck and is a consultant/advisory board member for Amgen, Roche, Sanofi, Bayer, Merck, and BMS. G. Bernhardt is a consultant/advisory board member for Morphosys AG. M.J. Smyth reports receiving a commercial research grant from Bristol Myers Squibb and Corvus Pharmaceuticals and other commercial research support from Arcus Biosciences. F. Kühnel reports receiving a commercial research grant from Mologen AG, Berlin, Germany. No potential conflicts of interest were disclosed by the other authors.

Authors' Contributions

Conception and design: S. Kubicka, E. Gürlevik, F. Kühnel
Development of methodology: J. Brooks, B. Fleischmann-Mundt, N. Woller, E. Gürlevik
Acquisition of data (provided animals, acquired and managed patients, provided facilities, etc.): J. Brooks, B. Fleischmann-Mundt, J. Niemann, S. Ribback, K. Peters, I.E. Demir, G.O. Ceyhan, G. Bernhardt, D.F. Calvisi
Analysis and interpretation of data (e.g., statistical analysis, biostatistics, computational analysis): J. Brooks, B. Fleischmann-Mundt, G.O. Ceyhan, S. Kubicka, M.J. Smyth, E. Gürlevik, F. Kühnel
Writing, review, and/or revision of the manuscript: J. Brooks, I.E. Demir, T.C. Wirth, G. Bernhardt, M.J. Smyth, D.F. Calvisi, F. Kühnel
Administrative, technical, or material support (i.e., reporting or organizing data, constructing databases): B. Fleischmann-Mundt, N. Woller, J. Niemann, I.E. Demir, N. Armbrecht, M.P. Manns
Study supervision: E. Gürlevik, F. Kühnel

Acknowledgments

F. Kühnel was supported by the Deutsche Forschungsgemeinschaft (TR209-C06 and KU2682/4-1), Deutsche Krebshilfe (109554), and Niedersächsische Krebsgesellschaft. E. Gürlevik was supported by the Deutsche Forschungsgemeinschaft (GU1508/1). M.J. Smyth was supported by the National Health and Medical Research Council of Australia Senior Principal Research Fellowship (1078671).

The costs of publication of this article were defrayed in part by the payment of page charges. This article must therefore be hereby marked *advertisement* in accordance with 18 U.S.C. Section 1734 solely to indicate this fact.

Received August 10, 2017; revised September 27, 2017; accepted November 7, 2017; published OnlineFirst November 27, 2017.

References

1. Fogel EL, Shahda S, Sandrasegaran K, DeWitt J, Easler JJ, Agarwal DM, et al. A multidisciplinary approach to pancreas cancer in 2016: a review. Am J Gastroenterol 2017;112:537–54.
2. Oettle H, Neuhaus P, Hochhaus A, Hartmann JT, Gellert K, Ridwelski K, et al. Adjuvant chemotherapy with gemcitabine and long-term outcomes among patients with resected pancreatic cancer: the CONKO-001 randomized trial. JAMA 2013;310:1473–81.
3. Evans DB, Varadhachary GR, Crane CH, Sun CC, Lee JE, Pisters PW, et al. Preoperative gemcitabine-based chemoradiation for patients with resectable adenocarcinoma of the pancreatic head. J Clin Oncol 2008; 26:3496–502.
4. Hodi FS, O'Day SJ, McDermott DF, Weber RW, Sosman JA, Haanen JB, et al. Improved survival with ipilimumab in patients with metastatic melanoma. N Engl J Med 2010;363:711–23.
5. Topalian SL, Hodi FS, Brahmer JR, Gettinger SN, Smith DC, McDermott DF, et al. Safety, activity, and immune correlates of anti-PD-1 antibody in cancer. N Engl J Med 2012;366:2443–54.
6. Liu J, Blake SJ, Yong MC, Harjunpaa H, Ngiow SF, Takeda K, et al. Improved efficacy of neoadjuvant compared to adjuvant immunotherapy to eradicate metastatic disease. Cancer Discov 2016;6:1382–99.
7. Carthon BC, Wolchok JD, Yuan J, Kamat A, Ng Tang DS, Sun J, et al. Preoperative CTLA-4 blockade: tolerability and immune monitoring in the setting of a presurgical clinical trial. Clin Cancer Res 2010;16: 2861–71.
8. Royal RE, Levy C, Turner K, Mathur A, Hughes M, Kammula US, et al. Phase 2 trial of single agent ipilimumab (anti-CTLA-4) for locally advanced or metastatic pancreatic adenocarcinoma. J Immunother 2010;33:828–33.

9. Eil R, Vodnala SK, Clever D, Klebanoff CA, Sukumar M, Pan JH, et al. Ionic immune suppression within the tumour microenvironment limits T cell effector function. Nature 2016;537:539–43.
10. Erez N, Truitt M, Olson P, Arron ST, Hanahan D. Cancer-associated fibroblasts are activated in incipient neoplasia to orchestrate tumor-promoting inflammation in an NF-kappaB-dependent manner. Cancer Cell 2010;17:135–47.
11. Nagaraj S, Gupta K, Pisarev V, Kinarsky L, Sherman S, Kang L, et al. Altered recognition of antigen is a mechanism of CD8+ T cell tolerance in cancer. Nat Med 2007;13:828–35.
12. Sutmuller RP, van Duivenvoorde LM, van EA, Schumacher TN, Wildenberg ME, Allison JP, et al. Synergism of cytotoxic T lymphocyte-associated antigen 4 blockade and depletion of CD25(+) regulatory T cells in antitumor therapy reveals alternative pathways for suppression of autoreactive cytotoxic T lymphocyte responses. J Exp Med 2001;194:823–32.
13. Bayne LJ, Beatty GL, Jhala N, Clark CE, Rhim AD, Stanger BZ, et al. Tumor-derived granulocyte-macrophage colony-stimulating factor regulates myeloid inflammation and T cell immunity in pancreatic cancer. Cancer Cell 2012;21:822–35.
14. Stromnes IM, Brockenbrough JS, Izeradjene K, Carlson MA, Cuevas C, Simmons RM, et al. Targeted depletion of an MDSC subset unmasks pancreatic ductal adenocarcinoma to adaptive immunity. Gut 2014; 63:1769–81.
15. Mitchem JB, Brennan DJ, Knolhoff BL, Belt BA, Zhu Y, Sanford DE, et al. Targeting tumor-infiltrating macrophages decreases tumor-initiating cells, relieves immunosuppression, and improves chemotherapeutic responses. Cancer Res 2013;73:1128–41.
16. Ene-Obong A, Clear AJ, Watt J, Wang J, Fatah R, Riches JC, et al. Activated pancreatic stellate cells sequester CD8+ T cells to reduce their infiltration of the juxtatumoral compartment of pancreatic ductal adenocarcinoma. Gastroenterology 2013;145:1121–32.
17. Beatty GL, Winograd R, Evans RA, Long KB, Luque SL, Lee JW, et al. Exclusion of T cells from pancreatic carcinomas in mice is regulated by Ly6C(low) F4/80(+) extratumoral macrophages. Gastroenterology 2015; 149:201–10.
18. Provenzano PP, Cuevas C, Chang AE, Goel VK, Von Hoff DD, Hingorani SR. Enzymatic targeting of the stroma ablates physical barriers to treatment of pancreatic ductal adenocarcinoma. Cancer Cell 2012;21:418–29.
19. Olive KP, Jacobetz MA, Davidson CJ, Gopinathan A, McIntyre D, Honess D, et al. Inhibition of Hedgehog signaling enhances delivery of chemotherapy in a mouse model of pancreatic cancer. Science 2009;324:1457–61.
20. Ozdemir BC, Pentcheva-Hoang T, Carstens JL, Zheng X, Wu CC, Simpson TR, et al. Depletion of carcinoma-associated fibroblasts and fibrosis induces immunosuppression and accelerates pancreas cancer with reduced survival. Cancer Cell 2014;25:719–34.
21. Chen DS, Mellman I. Oncology meets immunology: the cancer-immunity cycle. Immunity 2013;39:1–10.
22. Knocke S, Fleischmann-Mundt B, Saborowski M, Manns MP, Kuhnel F, Wirth TC, et al. Tailored tumor immunogenicity reveals regulation of CD4 and CD8 T cell responses against cancer. Cell Rep 2016;17: 2234–46.
23. Seth S, Maier MK, Qiu Q, Ravens I, Kremmer E, Forster R, et al. The murine pan T cell marker CD96 is an adhesion receptor for CD155 and nectin-1. Biochem Biophys Res Commun 2007;364:959–65.
24. Gurlevik E, Fleischmann-Mundt B, Brooks J, Demir IE, Steiger K, Ribback S, et al. Administration of gemcitabine after pancreatic tumor resection in mice induces an antitumor immune response mediated by natural killer cells. Gastroenterology 2016;151:338–50.
25. Webb JR, Milne K, Watson P, Deleeuw RJ, Nelson BH. Tumor-infiltrating lymphocytes expressing the tissue resident memory marker CD103 are associated with increased survival in high-grade serous ovarian cancer. Clin Cancer Res 2014;20:434–44.
26. Wang ZQ, Milne K, Derocher H, Webb JR, Nelson BH, Watson PH. CD103 and intratumoral immune response in breast cancer. Clin Cancer Res 2016;22:6290–7.
27. Le FA, Jalil A, Vergnon I, Le Maux CB, Lazar V, Bismuth G, et al. Alpha E beta 7 integrin interaction with E-cadherin promotes antitumor CTL activity by triggering lytic granule polarization and exocytosis. J Exp Med 2007;204: 559–70.
28. Suzuki E, Kapoor V, Jassar AS, Kaiser LR, Albelda SM. Gemcitabine selectively eliminates splenic Gr-1+/CD11b+ myeloid suppressor cells in tumor-bearing animals and enhances antitumor immune activity. Clin Cancer Res 2005;11:6713–21.
29. Gubin MM, Zhang X, Schuster H, Caron E, Ward JP, Noguchi T, et al. Checkpoint blockade cancer immunotherapy targets tumour-specific mutant antigens. Nature 2014;515:577–81.
30. Chan CJ, Martinet L, Gilfillan S, Souza-Fonseca-Guimaraes F, Chow MT, Town L, et al. The receptors CD96 and CD226 oppose each other in the regulation of natural killer cell functions. Nat Immunol 2014;15:431–8.
31. Peng YP, Xi CH, Zhu Y, Yin LD, Wei JS, Zhang JJ, et al. Altered expression of CD226 and CD96 on natural killer cells in patients with pancreatic cancer. Oncotarget 2016;7:66586–94.
32. Nishiwada S, Sho M, Yasuda S, Shimada K, Yamato I, Akahori T, et al. Clinical significance of CD155 expression in human pancreatic cancer. Anticancer Res 2015;35:2287–97.
33. Blake SJ, Stannard K, Liu J, Allen S, Yong MC, Mittal D, et al. Suppression of metastases using a new lymphocyte checkpoint target for cancer immunotherapy. Cancer Discov 2016;6:446–59.
34. Meyer D, Seth S, Albrecht J, Maier MK, du PL, Ravens I, et al. CD96 interaction with CD155 via its first Ig-like domain is modulated by alternative splicing or mutations in distal Ig-like domains. J Biol Chem 2009;284:2235–44.
35. Tai LH, Zhang J, Scott KJ, de Souza CT, Alkayyal AA, Ananth AA, et al. Perioperative influenza vaccination reduces postoperative metastatic disease by reversing surgery-induced dysfunction in natural killer cells. Clin Cancer Res 2013;19:5104–15.
36. Sanford DE, Belt BA, Panni RZ, Mayer A, Deshpande AD, Carpenter D, et al. Inflammatory monocyte mobilization decreases patient survival in pancreatic cancer: a role for targeting the CCL2/CCR2 axis. Clin Cancer Res 2013;19:3404–15.
37. Guerra C, Schuhmacher AJ, Canamero M, Grippo PJ, Verdaguer L, Perez-Gallego L, et al. Chronic pancreatitis is essential for induction of pancreatic ductal adenocarcinoma by K-Ras oncogenes in adult mice. Cancer Cell 2007;11:291–302.
38. Lesina M, Kurkowski MU, Ludes K, Rose-John S, Treiber M, Kloppel G, et al. Stat3/Socs3 activation by IL-6 transsignaling promotes progression of pancreatic intraepithelial neoplasia and development of pancreatic cancer. Cancer Cell 2011;19:456–69.
39. Baumgart S, Chen NM, Siveke JT, Konig A, Zhang JS, Singh SK, et al. Inflammation-induced NFATc1-STAT3 transcription complex promotes pancreatic cancer initiation by KrasG12D. Cancer Discov 2014;4:688–701.
40. Mazur PK, Herner A, Mello SS, Wirth M, Hausmann S, Sanchez-Rivera FJ, et al. Combined inhibition of BET family proteins and histone deacetylases as a potential epigenetics-based therapy for pancreatic ductal adenocarcinoma. Nat Med 2015;21:1163–71.
41. Poschke I, Faryna M, Bergmann F, Flossdorf M, Lauenstein C, Hermes J, et al. Identification of a tumor-reactive T cell repertoire in the immune infiltrate of patients with resectable pancreatic ductal adenocarcinoma. Oncoimmunology 2016;5:e1240859.
42. Jiang H, Hegde S, Knolhoff BL, Zhu Y, Herndon JM, Meyer MA, et al. Targeting focal adhesion kinase renders pancreatic cancers responsive to checkpoint immunotherapy. Nat Med 2016;22:851–60.
43. Rizvi NA, Hellmann MD, Snyder A, Kvistborg P, Makarov V, Havel JJ, et al. Cancer immunology. Mutational landscape determines sensitivity to PD-1 blockade in non-small cell lung cancer. Science 2015;348:124–8.
44. Snyder A, Makarov V, Merghoub T, Yuan J, Zaretsky JM, Desrichard A, et al. Genetic basis for clinical response to CTLA-4 blockade in melanoma. N Engl J Med 2014;371:2189–99.
45. Winograd R, Byrne KT, Evans RA, Odorizzi PM, Meyer AR, Bajor DL, et al. Induction of T cell immunity overcomes complete resistance to PD-1 and CTLA-4 blockade and improves survival in pancreatic carcinoma. Cancer Immunol Res 2015;3:399–411.
46. Lutz ER, Wu AA, Bigelow E, Sharma R, Mo G, Soares K, et al. Immunotherapy converts nonimmunogenic pancreatic tumors into immunogenic foci of immune regulation. Cancer Immunol Res 2014;2:616–31.
47. Dong H, Strome SE, Salomao DR, Tamura H, Hirano F, Flies DB, et al. Tumor-associated B7-H1 promotes T cell apoptosis: a potential mechanism of immune evasion. Nat Med 2002;8:793–800.
48. Taube JM, Anders RA, Young GD, Xu H, Sharma R, McMiller TL, et al. Colocalization of inflammatory response with B7-h1 expression in human melanocytic lesions supports an adaptive resistance mechanism of immune escape. Sci Transl Med 2012;4:127ra37.

49. Herbst RS, Soria JC, Kowanetz M, Fine GD, Hamid O, Gordon MS, et al. Predictive correlates of response to the anti-PD-L1 antibody MPDL3280A in cancer patients. Nature 2014;515:563–7.
50. Sainz B Jr, Alcala S, Garcia E, Sanchez-Ripoll Y, Azevedo MM, Cioffi M, et al. Microenvironmental hCAP-18/LL-37 promotes pancreatic ductal adenocarcinoma by activating its cancer stem cell compartment. Gut 2015;64:1921–35.
51. Aiello NM, Bajor DL, Norgard RJ, Sahmoud A, Bhagwat N, Pham MN, et al. Metastatic progression is associated with dynamic changes in the local microenvironment. Nat Commun 2016;7:12819.
52. Chan CJ, Andrews DM, McLaughlin NM, Yagita H, Gilfillan S, Colonna M, et al. DNAM-1/CD155 interactions promote cytokine and NK cell-mediated suppression of poorly immunogenic melanoma metastases. J Immunol 2010;184:902–11.